Clim Dyn (2010) 34:797–818
DOI 10.1007/s00382-008-0508-1

Relative contribution of soil moisture and snow mass to seasonal climate predictability: a pilot study

Hervé Douville

Received: 26 September 2008 / Accepted: 9 December 2008 / Published online: 16 January 2009

Abstract Land surface hydrology (LSH) is a potential source of long-range atmospheric predictability that has received less attention than sea surface temperature (SST). In this study, we carry out ensemble atmospheric simulations driven by observed or climatological SST in which the LSH is either interactive or nudged towards a global monthly re-analysis. The main objective is to evaluate the impact of soil moisture or snow mass anomalies on seasonal climate variability and predictability over the 1986–1995 period. We first analyse the annual cycle of zonal mean potential (perfect model approach) and effective (simulated vs. observed climate) predictability in order to identify the seasons and latitudes where land surface initialization is potentially relevant. Results highlight the influence of soil moisture boundary conditions in the summer mid-latitudes and the role of snow boundary conditions in the northern high latitudes. Then, we focus on the Eurasian continent and we contrast seasons with opposite land surface anomalies. In addition to the nudged experiments, we conduct ensembles of seasonal hindcasts in which the relaxation is switched off at the end of spring or winter in order to evaluate the impact of soil moisture or snow mass initialization. LSH appears as an effective source of surface air temperature and precipitation predictability over Eurasia (as well as North America), at least as important as SST in spring and summer. Cloud feedbacks and large-scale dynamics contribute to amplify the regional temperature response, which is however, mainly found at the lowest model levels and only represents a small fraction of the observed variability in the upper troposphere.

H. Douville (✉)
Météo-France/CNRM/GMGEC/UDC, 42 Avenue Coriolis,
31057 Toulouse Cedex 01, France
e-mail: herve.douville@meteo.fr

1 Introduction

Over recent decades, the recognition that slowly-evolving boundary conditions can be a source of atmospheric predictability at the seasonal timescale has promoted the development of coupled ocean-atmosphere general circulation models (GCMs) as well as the design of ocean data assimilation techniques (Palmer and Anderson 1994). Pilot studies such as the Development of a European Multimodel Ensemble system for seasonal to inTERannual prediction (DEMETER, Palmer 2005) project have demonstrated the potential of dynamical seasonal prediction (DSP) systems, which are now operated routinely by several countries. Nevertheless, it has been recently suggested that our ability to predict regional climate anomalies at the seasonal timescale has reached a plateau (WCRP 2008). While decadal prediction is now emerging as a new challenge for the global climate modeling community, the improvement of current DSP systems should not be relegated to a secondary objective.

In June 2007, the first WCRP Workshop on Seasonal Prediction was held in Barcelona to define a road-map for the next decade. On the one hand, it was recognized that the relative success of the multi-model ensemble forecasting (Doblas-Reyes et al. 2005) should not obviate the need of carrying on the development of coupled ocean–atmosphere GCMs and of ocean data assimilation techniques. On the other hand, it was highlighted that other components of the global climate system could contribute to improved forecast skill, and that "land–atmosphere

interactions are perhaps the most obvious example of the need to improve the representation of climate system interactions and their potential to improve forecast quality". While such a perspective is not new (Delworth and Manabe 1989; Dirmeyer 2000; Douville and Chauvin 2000; Koster et al. 2000), the lack of global land surface observations and of reliable land surface data assimilation techniques has been and still is a major obstacle for drawing robust conclusions on this issue.

In the mid-1990s, the International Satellite Land Surface Climatology Project (ISLSCP) has been launched and has allowed land surface modelers to produce global soil moisture climatologies by driving their models with common atmospheric forcings in the framework of the Global Soil Wetness Project (GSWP, http://grads.iges.org/gswp). The Interaction Soil–Biosphere–Atmosphere (ISBA, Mahfouf et al. 1995; Douville et al. 1995) land surface model of Centre National de Recherches Météorologiques (CNRM) has contributed to GSWP and has been driven by the ISLSCP data first from 1987 to 1988 (GSWP-1, Douville 1998), then from 1986 to 1995 (GSWP-2, Decharme and Douville 2007). Besides control runs using the common ISLSCP soil and vegetation parameters, parallel integrations have been achieved with the native ISBA land surface parameters to produce soil moisture and snow mass climatologies that are fully consistent with the CNRM atmospheric GCM. These climatologies have been used to nudge global atmospheric simulations and compare the relative influence of monthly soil moisture and SST on atmospheric variability and predictability at the seasonal timescale (Douville and Chauvin 2000; Douville 2002; Conil et al. 2007).

Consistent with former or parallel studies (i.e., Dirmeyer 2005), these sensitivity experiments have emphasized the relevance of soil moisture boundary conditions for capturing the interannual climate variability observed at the regional scale, particularly during the boreal summer season. Obviously, the strength and spatial distribution of the land-surface coupling is, however, model-dependent given the diversity of atmospheric GCMs. This issue was tackled by the global land–atmosphere coupling experiment (GLACE) intercomparison project (Koster and the GLACE team 2004) aimed at comparing where and to what extent boreal summer precipitation is controlled by soil moisture in a dozen of models. The results showed a large spread between the models, but highlighted three "hotspots" where the coupling appears as relatively strong in a majority of models: North America, Sahel and northern India. Nevertheless, the conclusions of GLACE should be considered with caution for at least three reasons. First, no observational counterpart of the coupling strength is available to confirm this distribution. Second, the metric that was used to measure the coupling strength was focused on subseasonal rather than seasonal variability. Third, the experiment design was based on seasonal hindcasts driven by the 1994 monthly SST and the results might have been somewhat different with another SST forcing.

The CNRM atmospheric GCM did not participate in GLACE, but also shows a significant precipitation sensitivity to soil moisture over the Sahel (Douville et al. 2001; Douville 2002) and North America (Douville 2004; Conil et al. 2007). In contrast with the results of GLACE, India does not appear as a region of strong coupling due to a negative dynamical feedback (less moisture convergence) that cancels the positive evaporation feedback over this region when the whole summer monsoon season is considered (Douville et al. 2001). Conversely, the CNRM model suggests that Europe is another region of strong coupling in summer (Douville and Chauvin 2000; Conil et al. 2007). This result is consistent with observational and numerical studies highlighting the potential contribution of soil moisture deficit to heat and drought waves over Western Europe (Ferranti and Viterbo 2006; Vautard et al. 2007), as well as with a recent statistical analysis of soil moisture feedbacks in the CMIP3 coupled ocean-atmosphere simulations (Notaro 2008). As far as the Sahel is concerned, Douville et al. (2007) highlighted the fact that the relatively strong coupling found in most GCMs (including in the CNRM model) does not guarantee a strong influence of soil moisture on the all-summer monsoon precipitation due to the dominant contribution of moisture convergence to the variability of rainfall (at least in the first part of the rainy season) and its strong sensitivity to the tropical SST.

Most studies do not tell much about the predictability of soil moisture itself and our ability to improve DSP systems through a better initialization of the LSH. To go one step further, Conil et al. (2008) have conducted additional ensembles of global atmospheric simulations driven by observed SST in which the soil moisture nudging is removed at the end of May in order to explore the impact of soil moisture initial conditions on summer hindcasts. Such experiments are similar to those formerly performed by Koster et al. (2004), but the focus is not limited to North America and to 1-month hindcasts. The results indicate that the CNRM atmospheric GCM is better than simple (autoregressive) statistical models for predicting the persistence of soil moisture anomalies. They also suggest that soil moisture memory is able to sustain a significant atmospheric predictability at the monthly to seasonal timescale.

The present article is the follow-on of Conil et al. (2007, 2008). Besides soil moisture, it also explores the influence of the Northern Hemisphere snow cover on atmospheric variability and predictability. Here again, former studies have been hampered by the lack of global observed climatologies (Kumar and Yang 2003). Visible imagery does

provide reliable estimates of the Northern Hemisphere snow cover since the late 1960s, but does not give access to snow depth anomalies. Off-line snow depth analyses have been recently produced (Brown et al. 2003), but not on the global scale. On-line NWP data assimilation techniques remain relatively crude and still show serious deficiencies when compared with in situ observations. Therefore, the nudging towards the monthly GSWP climatology developed by Douville and Chauvin (2000) again appears as an attractive strategy to prescribe "realistic" snow boundary conditions in the CNRM atmospheric model. Moreover, as in Conil et al. (2008), the nudging can be removed at the beginning of a particular season to explore the relevance of initial versus boundary conditions.

The experiment design is further described in Sect. 2. In Sect. 3, the annual cycle of predictability is compared between the control and nudged experiments. In Sect. 4, a regional and seasonal analysis, including the role of initial conditions, is conducted for particular years with contrasted land surface anomalies. The focus is on the Eurasian continent, which does not necessarily appear as a region of strong land-atmosphere coupling in former numerical studies. A summary and discussion of the results is given in Sect. 5.

2 Experiment design and predictability metrics

The Arpege-Climat atmospheric GCM coupled to the ISBA land surface model (Mahfouf et al. 1995; Douville et al. 1995) has been used to perform global seasonal hindcasts in which soil moisture or snow mass is either interactive or strongly relaxed towards a monthly reanalysis. The reanalysis covers the 1986–1995 period and has been produced by driving the ISBA model with a combination of 3-hourly atmospheric analyses and of monthly climatologies based on in situ and satellite observations (Dirmeyer et al. 2006; Decharme and Douville 2007). In both off-line and on-line configurations, ISBA here uses a single-layer snow model (Douville et al. 1995) and a simple force-restore soil hydrology with a Variable Infiltration Capacity runoff scheme. The GSWP-2 reanalysis is first used to nudge either soil moisture or snow mass in ensembles of AMIP-type simulations, i.e., global atmospheric simulations driven by observed monthly mean SST. Then climatological rather than observed monthly mean SST are prescribed to isolate the land surface contribution to climate variability. Finally, the impact of land surface initialization is explored by removing the nudging at the beginning of seasonal hindcasts driven by observed SST.

Table 1 summarizes the various experiments. Most ensembles consist of ten integrations from 1st September 1985 to 31st December 1995. The different initial conditions are derived from 10 consecutive years of a pre-existing AMIP-type experiment. The first 4 months of each member are considered as a spin-up and no attention is paid to the impact of atmospheric initialization on seasonal predictability. In the control case (FF), there is no nudging so that soil moisture and snow mass are fully interactive with the atmosphere. In a first pair of sensitivity experiments (GG and HH), soil moisture and snow mass, respectively, are nudged towards the GSWP-2 reanalysis interpolated onto the model grid and averaged on a monthly basis. Then, parallel experiments (GC and HC) have been performed with climatological SST (mean annual cycle averaged over the 1986–1995 period) to evaluate the robustness of the results and the additivity of the oceanic and land surface contributions to seasonal predictability. Finally, two ensembles of seasonal hindcasts using an interactive LSH and prescribed observed SST (GF and HF) have been performed to assess the impact of initial rather than boundary conditions of soil moisture and snow mass. Each of the ten integrations for each of the 10 years (1986–1995) starts from GG and HH initial conditions, respectively, either at the end of May (GF, impact of soil moisture initialization on boreal summer hindcasts) or at the end of March (HF, impact of snow mass initialization on boreal spring hindcasts).

Further technical details on the nudging technique can be found in Douville (2003). The nudged soil moisture experiments have been already compared to the control ensemble by Conil et al. (2007). The influence of soil moisture initialization on summer hindcasts has been also

Table 1 Summary of the experiments

Expt	SST	Soil moisture	Snow mass
FF	AMIP	Free	Free
GG	AMIP	Nudged toward GSWP-2	Free
HH	AMIP	Free	Nudged toward GSWP-2
GC	AMIP monthly climatology	Nudged toward GSWP-2	Free
HC	AMIP monthly climatology	Free	Nudged toward GSWP-2
GF	AMIP (June to September)	Initialized from GG in late May then free	Free
HF	AMIP (April to September)	Free	Initialized from HH in late March then free

explored by Conil et al. (2008). These results are further discussed in the continuation of the present study and are compared to the impacts of snow boundary conditions and of snow initialization. Note again that none of these experiments deals with the impact of atmospheric initialization, which however, can be important during the first month of the simulations. Such an experiment design allows us to focus only on the impact of the land surface initialization in the GF and HF experiments.

Two metrics have been used to quantify predictability in the various experiments. We have first conducted a one-way analysis of variance (ANOVA) to evaluate *potential* predictability (hereafter PP) and its relative sensitivity to LSH and SST boundary conditions. This technique allows us to split the total variance of the CNRM model into a chaotic internal component and an external component driven by the lower boundary conditions (Douville 2004). Details on the methodology and its underlying hypotheses can be found in Von Storch and Zwiers (1999). In this perfect-model approach, PP is the ratio of external versus total variability. The total variance is estimated from the 100 seasonal integrations each experiment consists of, while the externally forced variance ignores the contribution of the atmospheric initial conditions and is computed from the ten ensemble mean seasons (from 1986 to 1995).

This idealized framework is here justified by the use of soil moisture and snow mass boundary conditions that are not derived directly from observations but are calculated by a land surface model. The gap between potential and effective predictability is therefore not entirely due to model deficiencies, but also to the inherent limitations of the GSWP-2 climatology. *Effective* predictability or model skill has been here simply measured as the temporal Anomaly Correlation Coefficient (ACC) between the simulated climate anomalies and those from the Climate Research Unit version 2 (CRU2, http://www.cru.uea.ac.uk/cru/data/) climatology after interpolation onto the GCM horizontal grid.

Given the 10-year framework of the study, such a skill score is obviously not robust. Comparing the PP and ACC distributions is thus important to distinguish between spurious and genuine peaks of effective predictability. A common assumption is indeed that PP represents an upper limit of effective predictability. While this hypothesis is not necessarily valid (since there is no guarantee that the signal to noise ratio is correct in the model), high PP is a necessary condition for the model to show some skill and PP is therefore very useful to detect high ACCs which are due to a stochastic artefact.

3 Annual cycle of zonal mean predictability

Another way to reduce the stochastic noise associated with the limited 10-year sampling is to show zonal mean rather than grid-point values of predictability. This is done in Fig. 1 which shows the impact of the nudging on the annual cycle of total variability, PP and ACC for surface air temperature over land areas comprised between 55°S and 75°N. Not surprisingly, the control experiment shows a maximum variability in the winter extratropics and minimum values in the Tropics. The distribution is not much sensitive to the nudging and only shows a weak decrease in total variability when using climatological rather than observed SST.

Moving to PP, the control experiment shows as expected maximum predictability in the Tropics where SST exerts a strong impact on atmospheric variability. Large values are also found in the Southern Hemisphere due to the limited number of land grid points and to the strong SST forcing in coastal regions. Conversely, PP remains all year round fairly limited in the northern extratropics. This feature is however very sensitive to the land surface boundary conditions. The soil moisture nudging (GG) increases PP in the boreal summer mid-latitudes, while the snow mass nudging (HH) has a similar impact during the springtime snowmelt and, though to lesser extent, at the beginning of the snow season. Such a sensitivity is confirmed by the results of GC and HC, which show consistent PP signals in the northern extratropics despite the use of climatological SST. This result suggests that the SST and LSH forcings are relatively additive in our experiments for these regions. Note however that both sources of atmospheric variability are not necessarily independent in the real world.

The last column in Fig. 1 shows the annual cycle of zonal mean effective predictability. In line with the PP distribution and with the results of operational DSP systems, the control experiment shows maximum skill scores in the Tropics. The ACC distribution is relatively noisy in the extratropics, but shows correlations that are generally less than 0.3. The nudged experiments show patches of higher predictability in which we are relatively confident given their consistency with the response of PP. The relevance of soil moisture boundary conditions (GG and GC) in the boreal summer mid-latitudes is confirmed. The impact of snow boundary conditions (HH and HC) in the northern extratropics is also found, but is apparently stronger in fall and winter than in spring. This apparent discrepancy with the response of PP might be explained by at least two factors. On the one hand, zonal mean ACC provide a biased estimate of predictability because of the limited 10-year period of the study. On the other hand, the spring peak of zonal mean PP could be related to a delayed snowmelt in the ISBA model (Decharme and Douville 2007) which could artificially inflate the potential predictability of surface air temperature in this particular season.

As far as land precipitation is concerned (Fig. 2), all experiments show a robust annual cycle of interannual

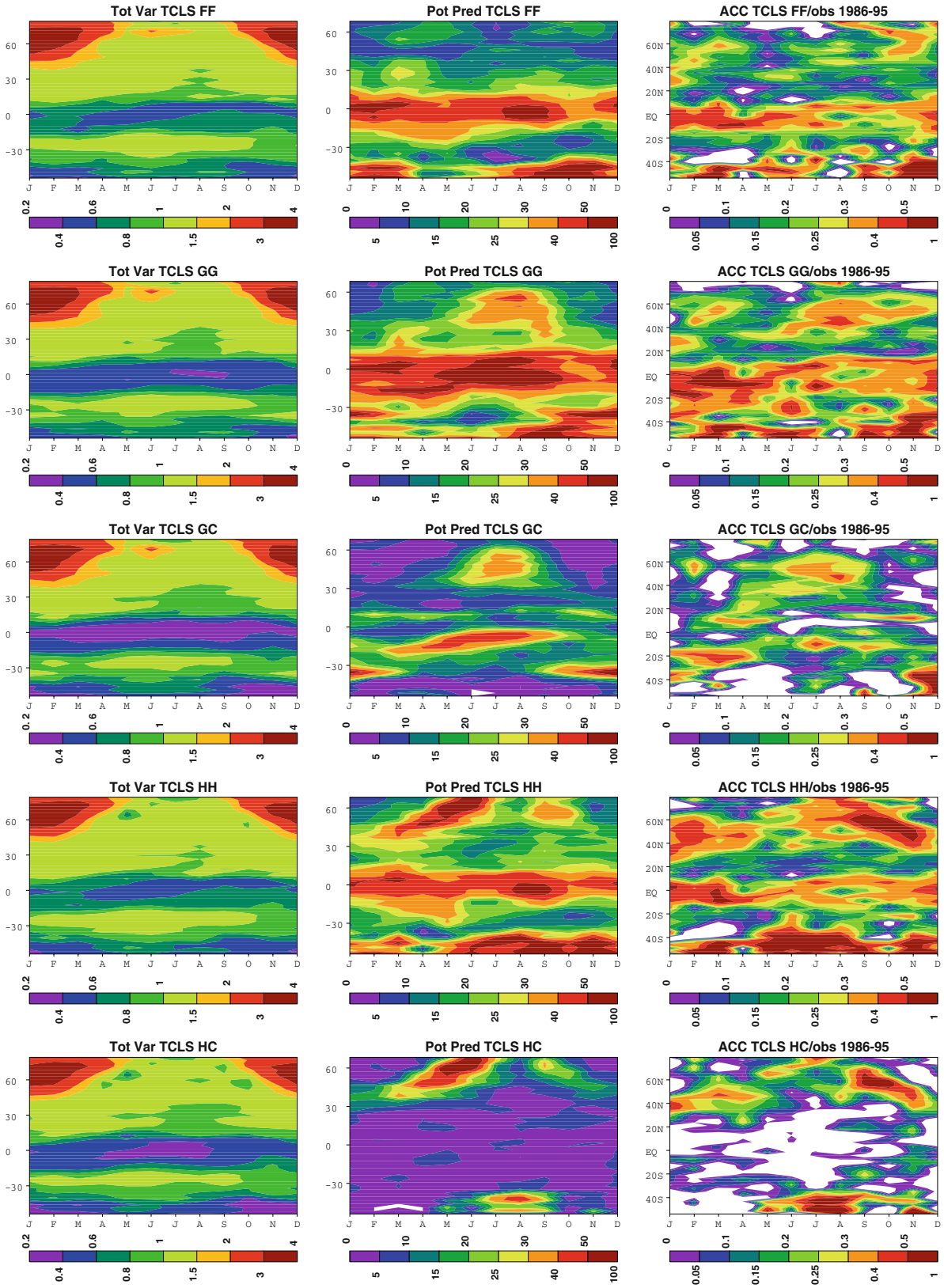

Fig. 1 Zonal mean annual cycle of land surface air temperature: interannual standard deviation (*left column*, in K), potential predictability (*central column*, in %) and effective predictability against the CRU2 climatology (*right column*, dimensionless ACC) in FF, GG, HH, GC and HC, respectively

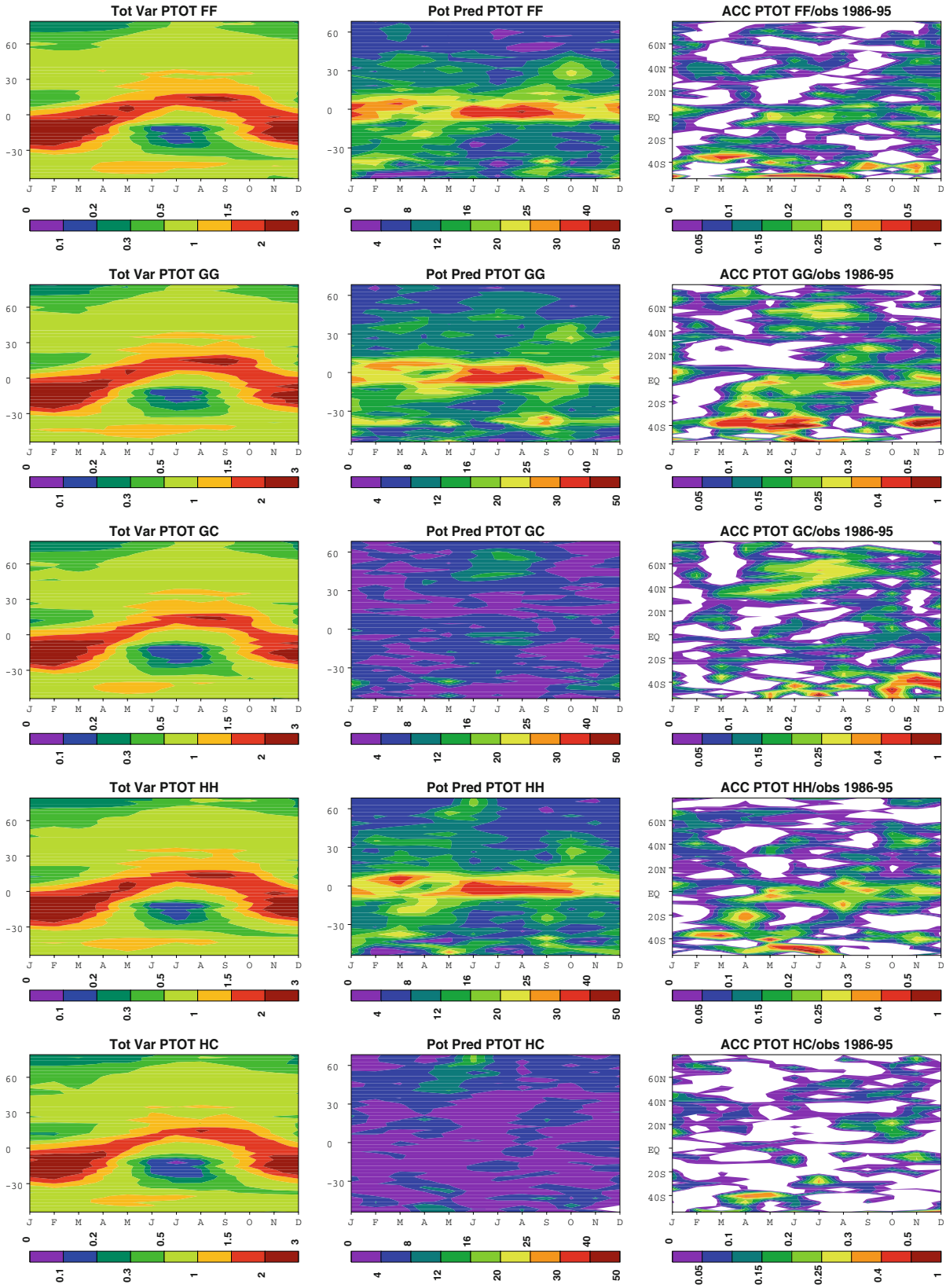

Fig. 2 Zonal mean annual cycle of land precipitation: interannual standard deviation (*left column*, in mm/day), potential predictability (*central column*, in %) and effective predictability against the CRU2 climatology (*right column*, dimensionless ACC) in FF, GG, HH, GC and HC, respectively

variability with maximum values following the seasonal migration of the inter-tropical convergence zone (ITCZ). In the control experiment, PP is found in the Tropics, but is much less than for surface air temperature and is very weak in the extratropics. Nudging soil moisture (snow mass) leads to a significant but limited increase in PP in the boreal summer mid-latitudes (boreal spring mid- and-high latitudes), that is found with or without SST forcing. In line with the low values of PP, the zonal mean ACC distribution is too noisy to get a robust evaluation of the effective predictability. Nonetheless, a peak of predictability appears in the boreal summer mid-latitudes when the soil moisture nudging is activated. This maximum is even more pronounced in GC than in GG, suggesting that the summer SST forcing not only does not represent a source of effective predictability in this region, but could even exert a spurious influence on the precipitation variability in the CNRM model due to a poor simulation of tropical-extratropical SST teleconnections.

4 Seasonal contrasts over Eurasia

We now concentrate on contrasted seasons, when the potential contribution of LSH to seasonal climate predictability is presumably the strongest over the 1986–1995 period. In addition to the former experiments with prescribed land surface boundary conditions, the impact of land surface initialization is also explored. The focus is on Eurasia that contributes to the zonal belt of increased predictability in Figs. 1 and 2. Despite its larger area, Eurasia has been less emphasized than North America as a region of strong soil moisture feedback. Moreover, it shows an extensive winter snow cover which is also likely to contribute to seasonal predictability.

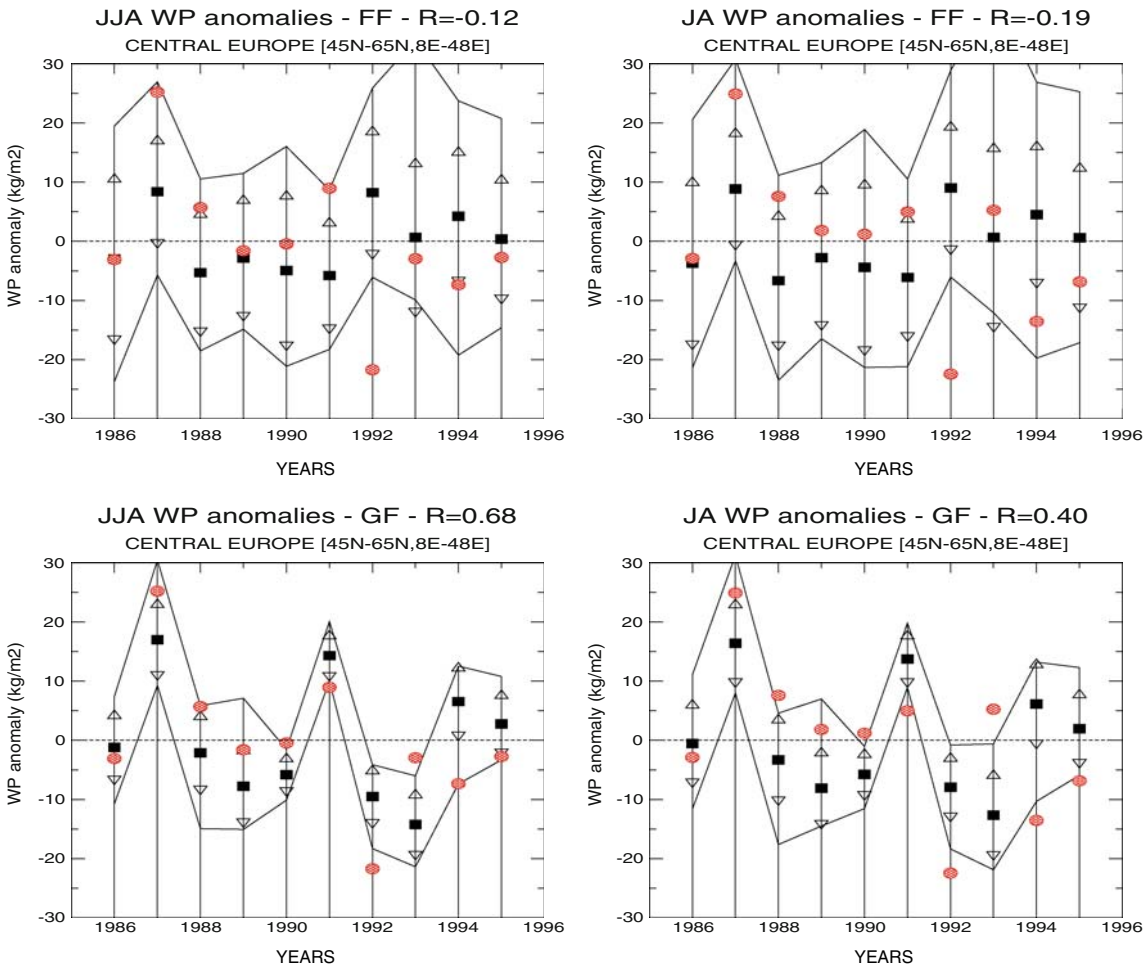

Fig. 3 June to August (JJA, *left panels*) and July to August (JA, *right panels*) soil moisture anomalies (kg/m^2) averaged over Central Europe from 1986 to 1995. Ensemble mean anomalies (*black squares*) simulated in the control (FF, *upper panels*) and seasonal hindcast (GF, *lower panels*) experiments are compared to GSWP-2 anomalies (*red disks*). For each experiment, R is the 10-year correlation of the ensemble mean values with the observations, *triangles* show ±1 standard deviation and solid lines correspond to the minimum and maximum anomalies

4.1 Predictability of soil moisture and snow mass

A first condition to be filled for the lower boundary conditions to play a role in seasonal climate prediction is the predictability of this lower boundary forcing itself. A second related condition is the presence of anomalies with a sufficient magnitude and spatial extent in the initial conditions. For this reason, the predictability of the LSH is here illustrated by focusing on two specific regions: Central Europe [45–65°N/8–48°E] for summer soil moisture and Central Eurasia [40–70°N/50–90°E] for spring snow mass.

Figures 3 and 4 compare the ensemble mean anomalies simulated over these regions in the control (FF) and seasonal hindcast (GF or HF) experiments to the GSWP-2 anomalies, relative to their respective 1986–1995 climatology. While again a 10-year period is too short to derive robust correlations, the contrasted spread and predictability found between FF on the one hand and GF or HF on the other hand is sufficient to draw the following conclusions. Firstly, the predictability of the LSH is very poor in the control experiment. This result indicates that the SST forcing is weak or even wrong (ex: summer 1992) in the model. Secondly, the spread is clearly reduced and the correlation is strongly improved in the seasonal hindcasts, suggesting a significant predictability of soil moisture and snow mass at the seasonal timescale. This predictability is also found when focusing on months 2–3 (right panels) and is therefore not limited to the first month after initialization. Such a persistence could be even more obvious in a more realistic set-up including analysed rather than random atmospheric initial conditions.

Figures 3 and 4 allow us to select two pairs of summer (1987 vs. 1992) and spring (1993 vs. 1995) seasons to

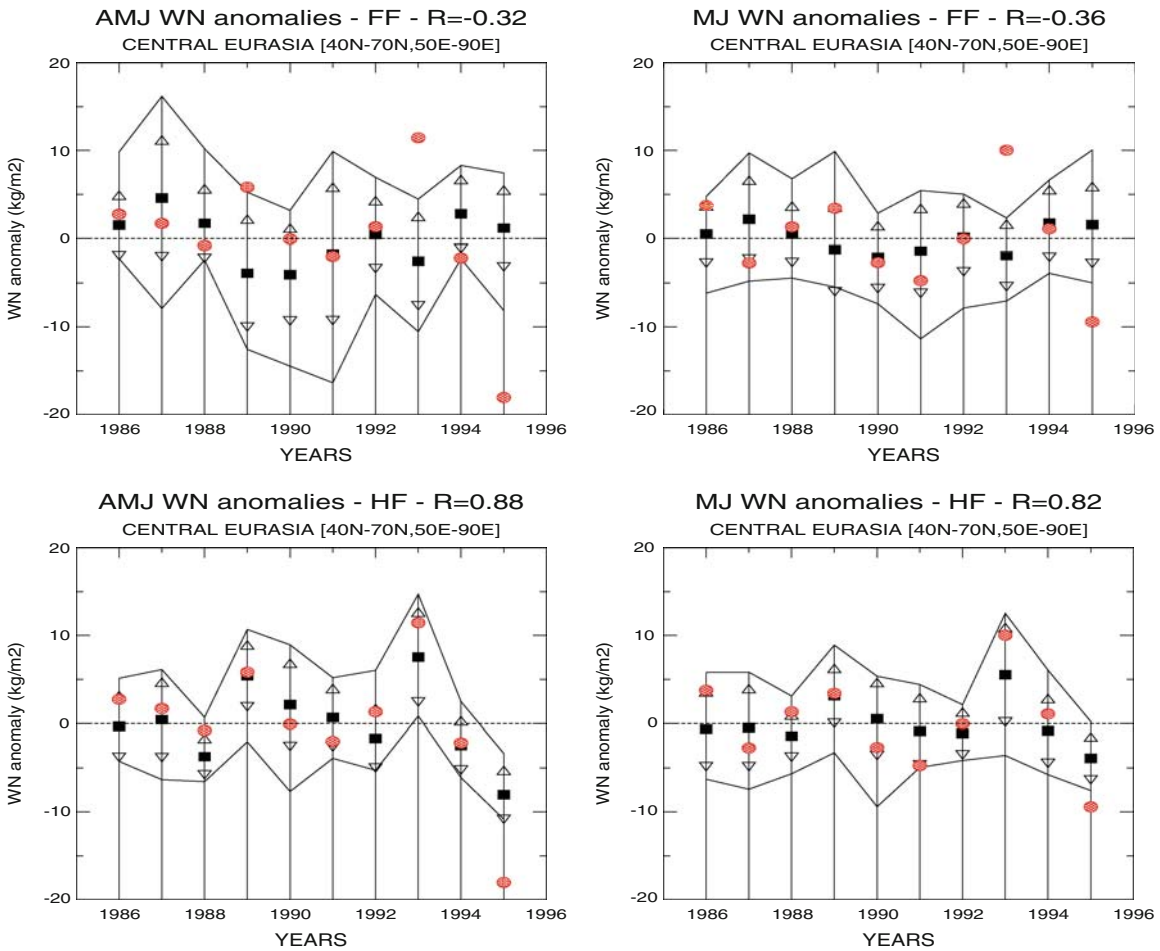

Fig. 4 April to June (AMJ, *left panels*) and May to June (MJ, *right panels*) snow mass anomalies (kg/m^2) averaged over Central Eurasia from 1986 to 1995. Ensemble mean anomalies (*black squares*) simulated in the control (FF, *upper panels*) and seasonal hindcast (HF, *lower panels*) experiments are compared to GSWP-2 anomalies (*red disks*). For each experiment, R is the 10-year correlation of the ensemble mean values with the observations, *triangles* show ±1 standard deviation and solid lines correspond to the minimum and maximum anomalies

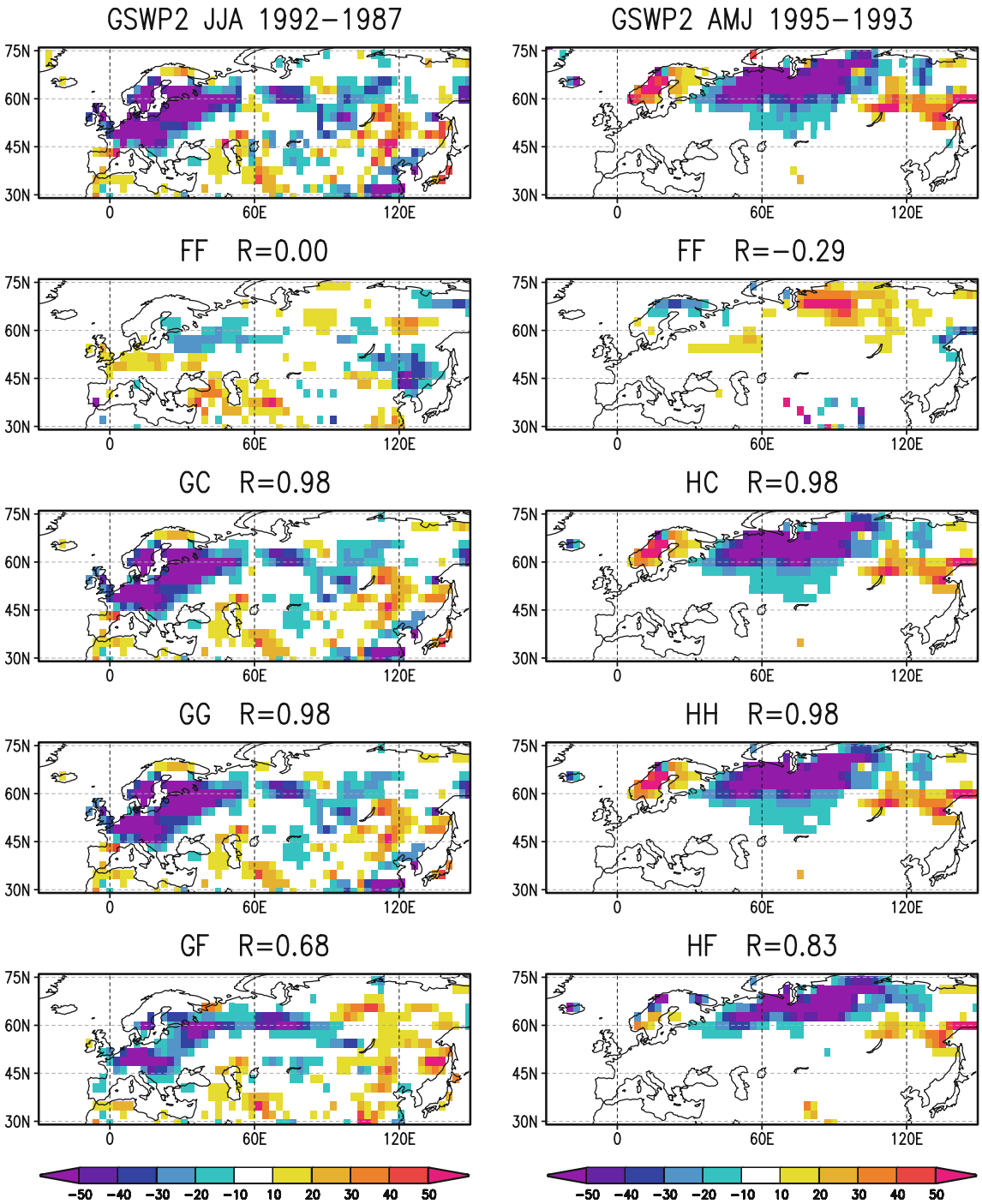

Fig. 5 *Left* June to August 1992 minus 1987 differences of soil moisture (kg/m^2) in FF, GC, GG and GF, respectively. *Right* April to June 1995 minus 1993 differences of snow mass (kg/m^2) in FF, HC, HH and HF, respectively. For each experiment, R is the spatial correlation with the upper panel (GSWP-2 reanalysis)

illustrate the impact of soil moisture and snow mass on climate predictability. For soil moisture, 1992 minus 1987 (left panels in Fig. 5) shows a strong deficit from June to August (JJA) over Europe that has been already emphasized by Conil et al. (2007, 2008). While such a deficit is not reproduced in the control experiment in spite of the observed SST forcing, it is perfectly imposed in GG and GC due to the nudging towards the GSWP-2 climatology. It is also partly captured in GF showing the predictability of soil moisture at the seasonal timescale when GSWP-2 is only used to initialize the model at the end of May. As far as snow is concerned, 1995 minus 1993 (right panels in

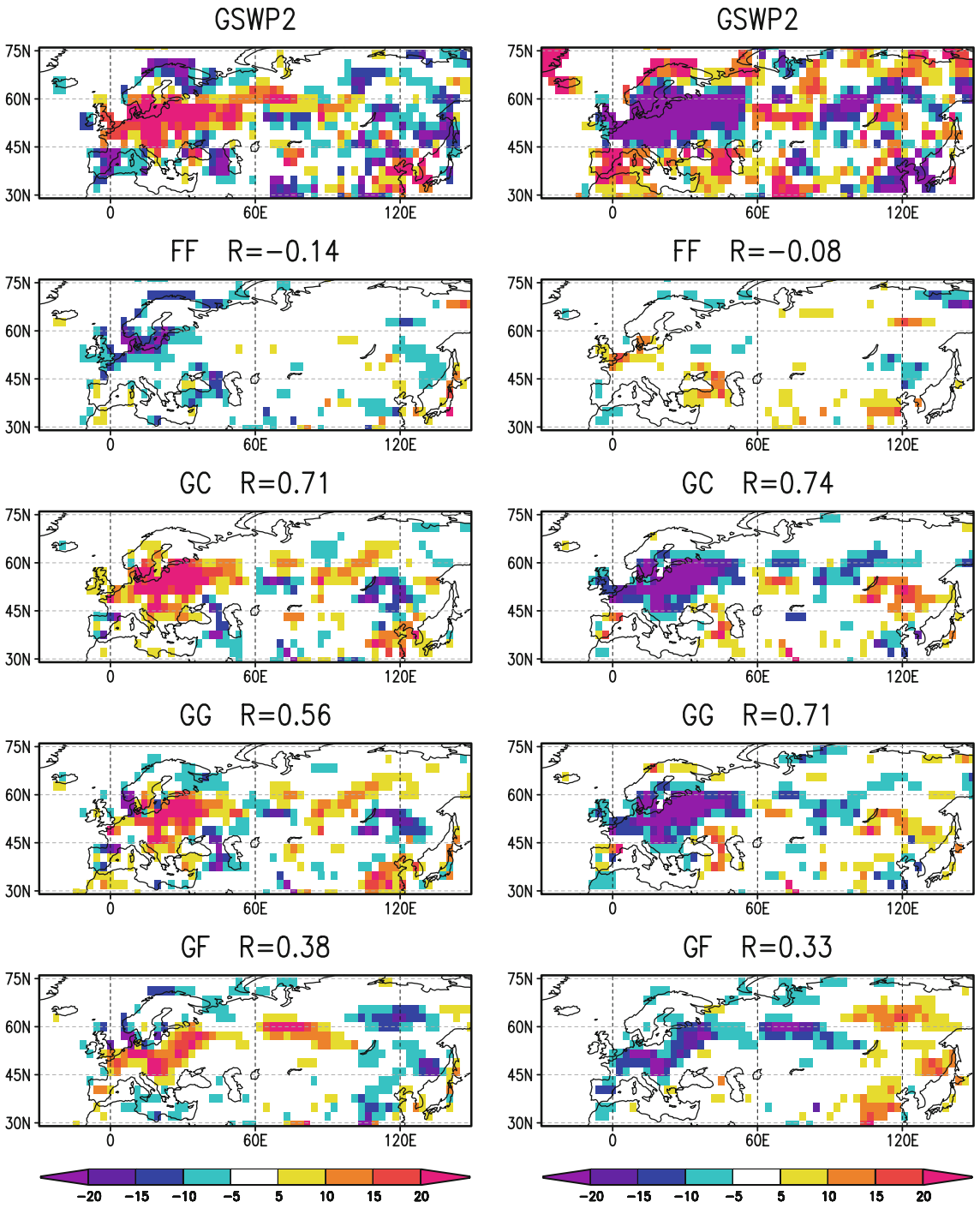

Fig. 6 June to August 1992 minus 1987 differences of surface latent (*left*) and sensible (*right*) heat fluxes (downward is positive, W/m^2) in FF, GC, GG and GF, respectively. For each experiment, R is the spatial correlation with the upper panel (GSWP-2 reanalysis)

Fig. 5) shows a strong deficit from April to June (AMJ) over central Eurasia, which is not found in the control experiment, correctly imposed in the nudged experiments (HC and HH) and relatively predictable when GSWP-2 is just used to initialize the model.

Such contrasted seasons are therefore particularly interesting to look at the land surface influence on atmospheric predictability. Note however that we do not claim that the land surface boundary conditions are really *perfect* in the nudged experiments: they are just as good as the GSWP-2 reanalysis, but they are perfectly consistent with the CNRM atmospheric GCM given the common use of the ISBA land surface model in the off-line GSWP-2 simulations and in the present study.

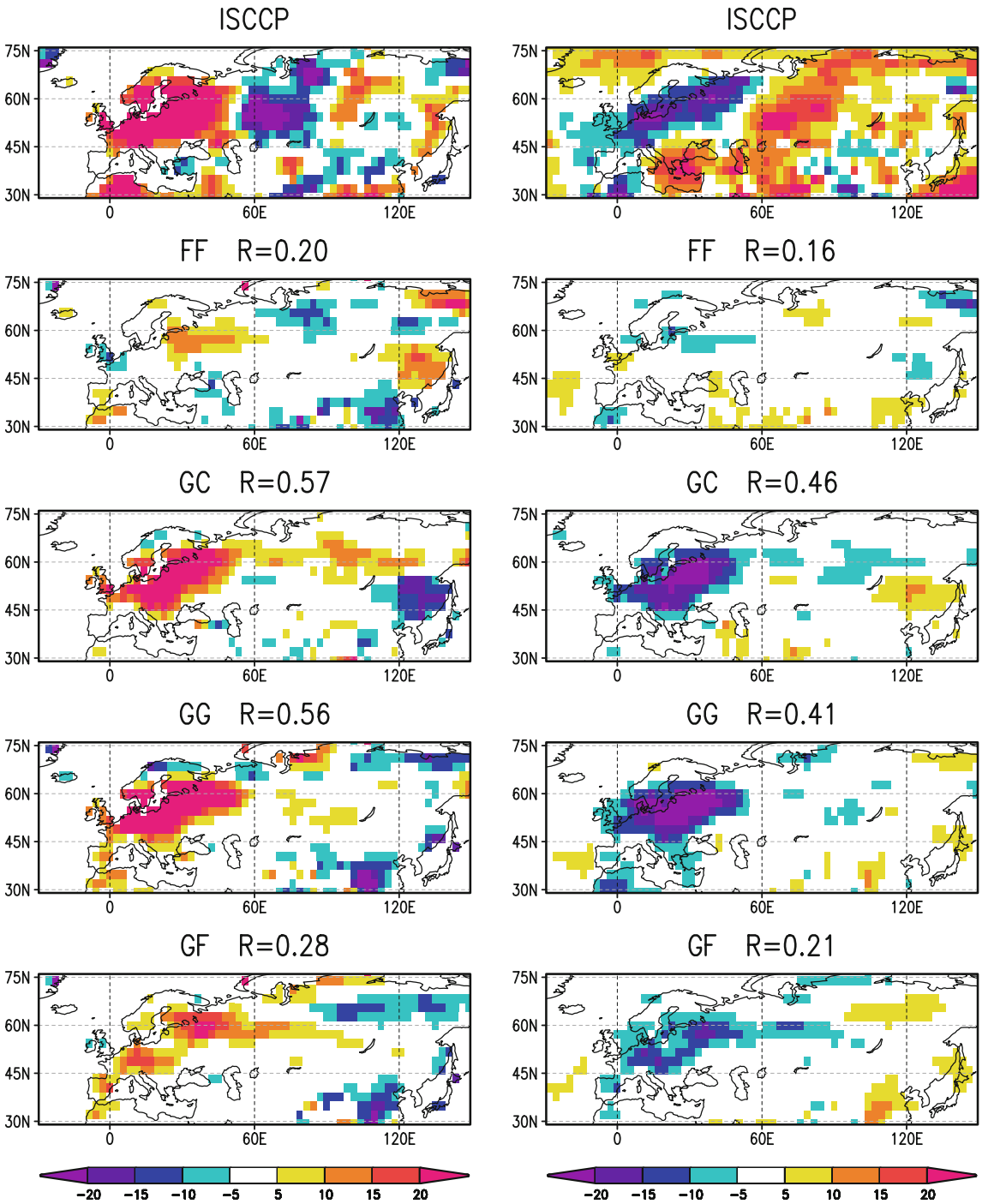

Fig. 7 June to August 1992 minus 1987 differences of surface net shortwave (*left*) and net longwave (*right*) radiation (downward is positive, W/m^2) in FF, GC, GG and GF, respectively. For each experiment, R is the spatial correlation with the upper panel (ISCCP2 climatology)

4.2 JJA 1992 minus JJA 1987

Looking first at the impact of soil moisture in summer, Fig. 6 compares the differences in the latent/sensible heat flux simulated in FF, GC, GG and GF with GSWP-2 (after interpolation onto the GCM horizontal grid). Not surprisingly, the soil moisture deficit is associated with a strong change in the Bowen ratio over Europe that is well captured in the nudged experiments (GC and GG) and also relatively consistent with GSWP-2 in the seasonal hincasts (GF). Figure 7 compares the simulated differences in net surface shortwave and longwave radiation against the International Satellite Cloud Climatology Project (ISCCP). This dataset indicates that the 1992 minus 1987 soil moisture deficit is

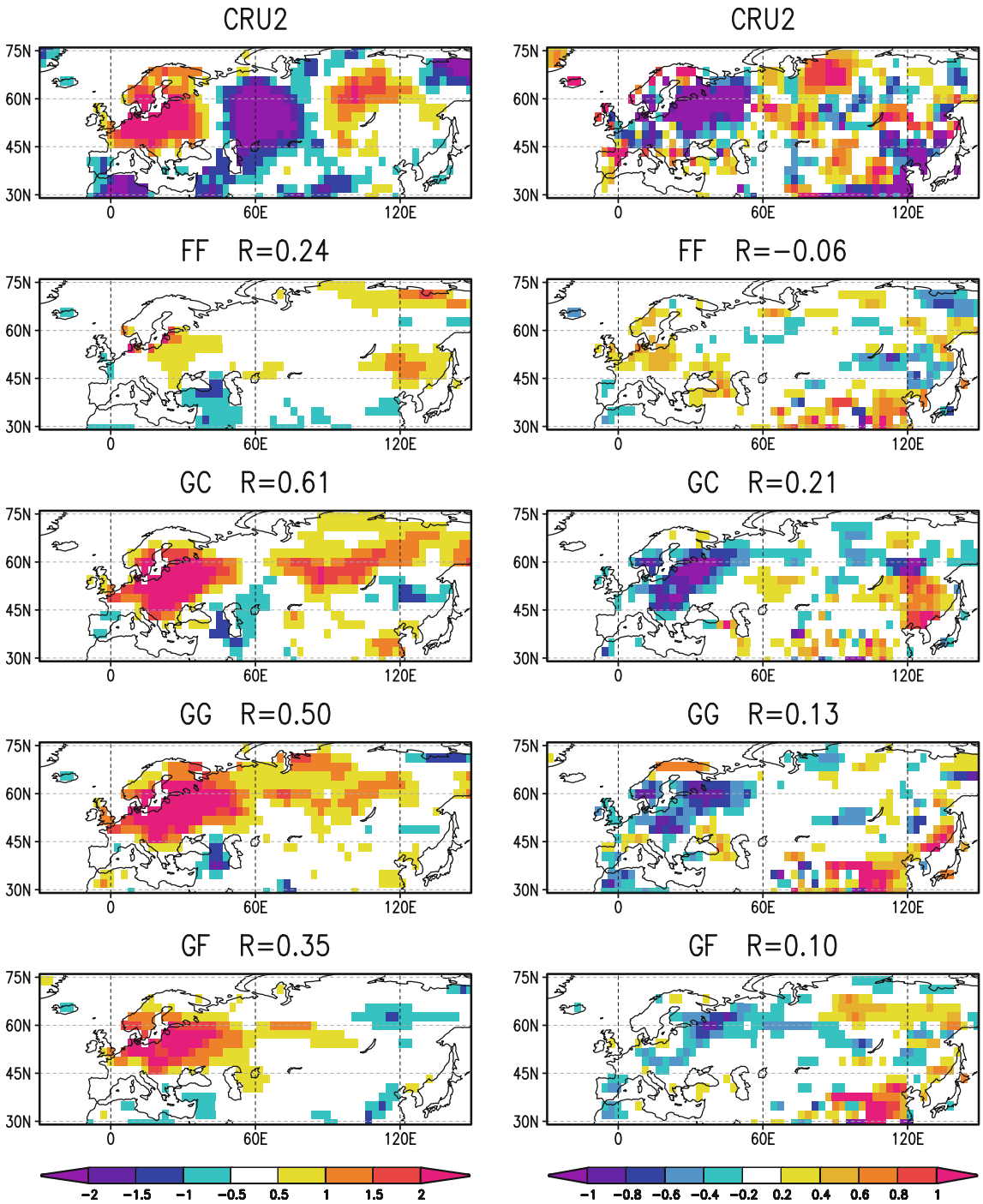

Fig. 8 June to August 1992 minus 1987 differences of surface air temperature (*left*, K) and precipitation (*right*, mm/day) in FF, GC, GG and GF, respectively. For each experiment, R is the spatial correlation with the upper panel (CRU2 climatology)

associated with an increase in net shortwave radiation and a decrease in net longwave radiation. Such anomalies are captured in the nudged experiments and are still visible in the seasonal hindcasts. They are associated with a significant decrease in total cloud cover which is indeed observed (not shown) in the ISCCP climatology and in the ERA40 reanalysis (Uppala et al. 2005).

In line with the response of the surface energy budget, the CRU2 climatology shows a strong warming and a precipitation deficit over Europe (Fig. 8). The temperature anomalies are weak and poorly simulated in the control experiment. In contrast, the warming is correctly simulated in the nudged experiments. The seasonal hindcasts also show a significant improvement compared to the control

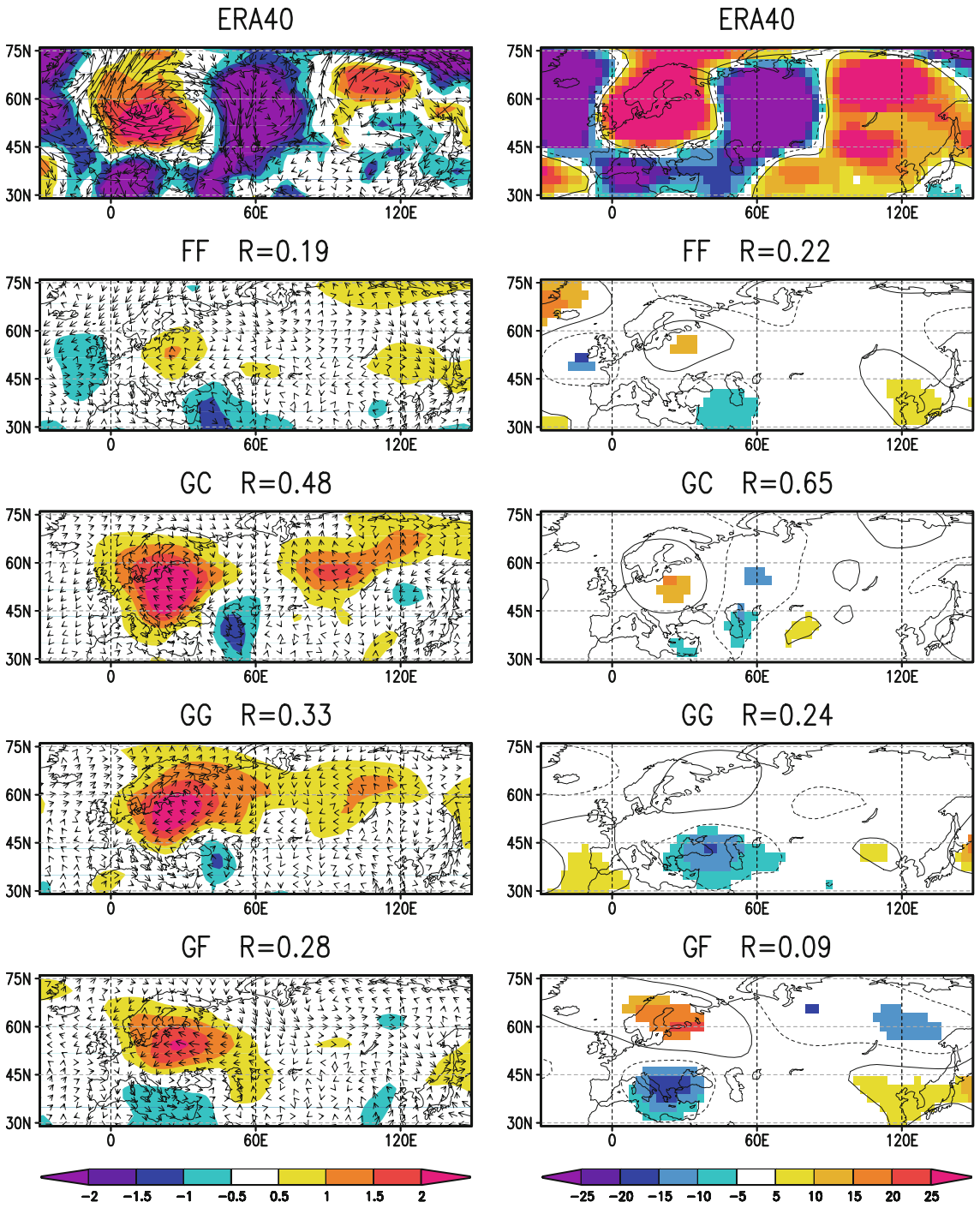

Fig. 9 June to August 1992 minus 1987 differences of temperature at 850 hPa (*left*, K) and geopotential eddy component at 500 hPa (*right*, m) in FF, GC, GG and GF, respectively. For each experiment, R is the spatial correlation with the upper panel (ERA40 reanalysis). *Left panels* horizontal wind vector anomalies at 850 hPa are superimposed on temperature differences. *Right panels black contours* denote the ±5 m *isolines* and *shading* show simulated differences that are statistically significant at a 5% level

case, thereby emphasizing the benefit from a better initialization of soil moisture. The same conclusions apply to the precipitation differences, even if the spatial correlation with the observed anomalies is systematically lower than for surface air temperature given the stronger magnitude and finer scale of precipitation variability.

As emphasized in Douville and Chauvin (2000) and Conil et al. (2007), the temperature sensitivity to the soil moisture forcing is not confined to the land surface and the precipitation sensitivity is not limited to a simple evaporation feedback. Figure 9 shows the simulated differences in temperature and wind vectors at 850 hPa, as well as the

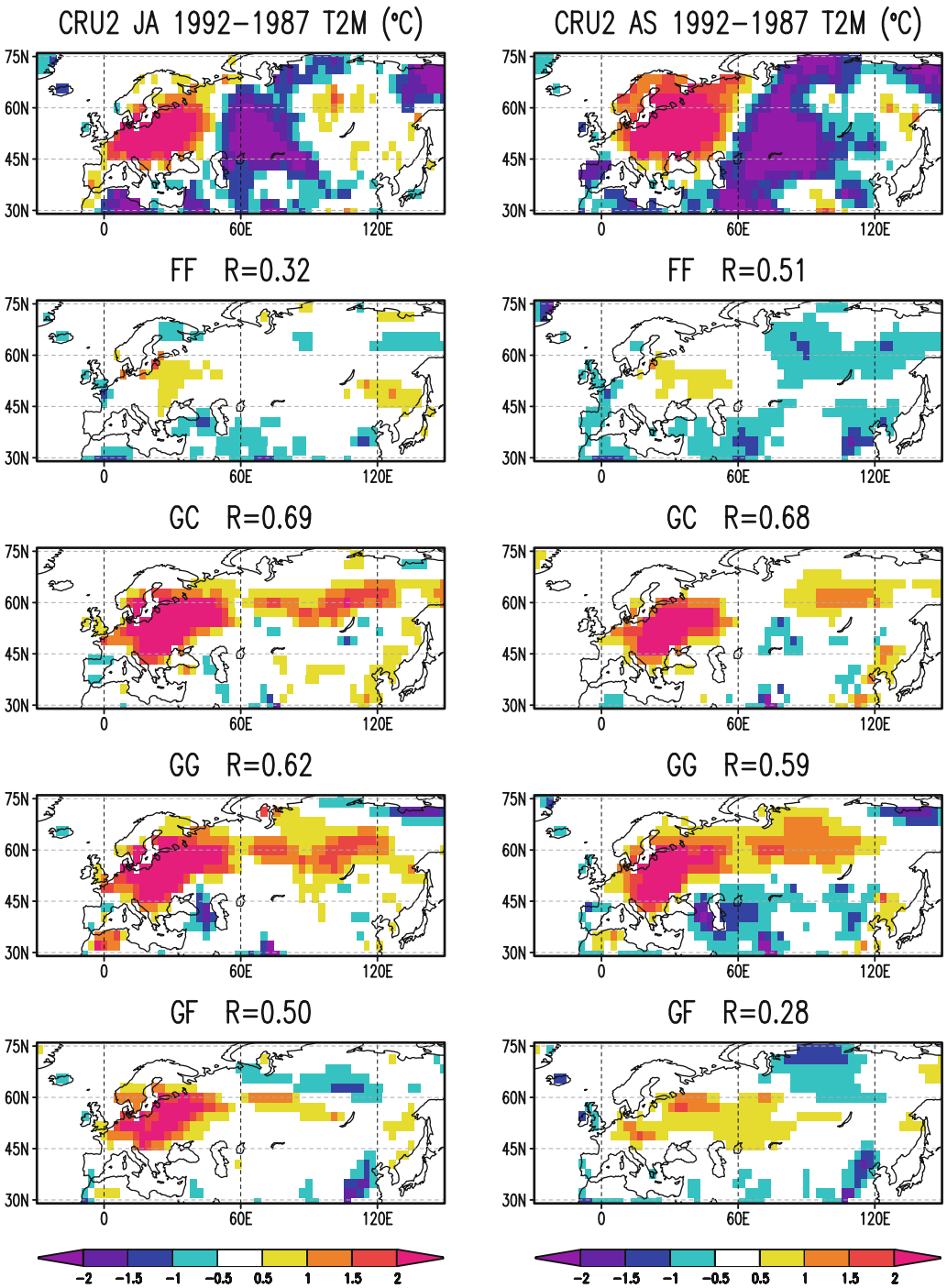

Fig. 10 July–August (JA, *left*) and August–September (AS, *right*) 1992 minus 1987 differences of surface air temperature (K) in FF, GC, GG and GF, respectively. For each experiment, R is the spatial correlation with the upper panel (CRU2 climatology)

eddy component of the 500 hPa geopotential height (Z500* which is obtained after removing the zonal mean values). The comparison of GC and FF first suggests that the soil moisture forcing is as strong as the SST forcing in the free troposphere (above the planetary boundary layer). The comparison with the ERA40 reanalysis also confirms our former hypothesis whereby the SST forcing could have a spurious influence on the extratropical circulation simulated by the CNRM atmospheric GCM. The maximum correlation with ERA40 is obtained in GC rather than in GG, emphasizing the dominant and more useful soil moisture forcing in the model. Moreover, the results

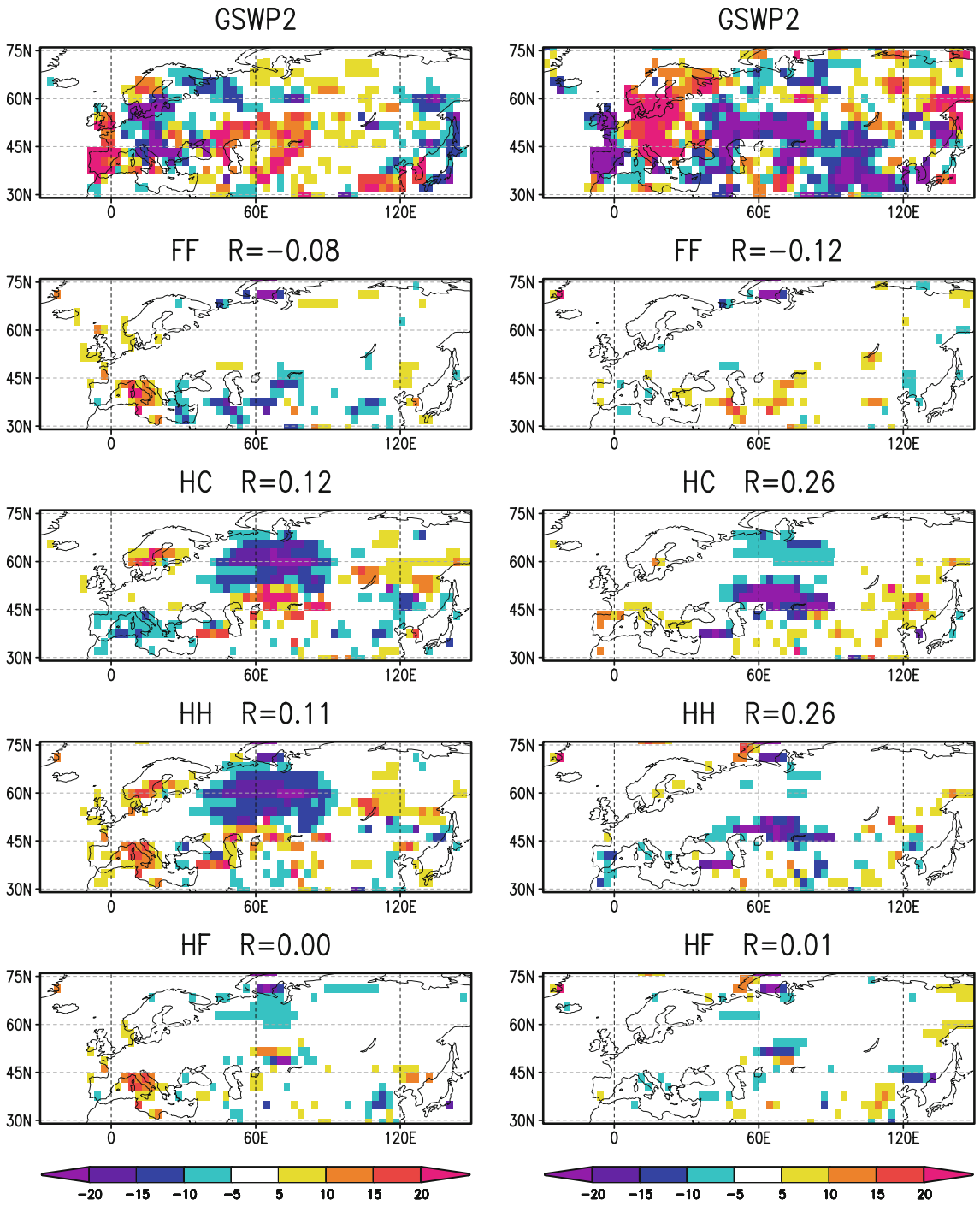

Fig. 11 April to June 1995 minus 1993 differences of surface latent (*left*) and sensible (*right*) heat fluxes (downward is positive, W/m^2) in FF, HC, HH and HF, respectively. For each experiment, R is the spatial correlation with the upper panel (GSWP-2 reanalysis)

suggest a large-scale dynamical response to the regional soil moisture deficit that is also found in the seasonal hindcasts but is underestimated in all experiments. This underestimation might be due to the smoothing effect of the ensemble mean calculation (only the predictable counterpart of the observed pattern is shown), but could also denote a lack of sensitivity of the CNRM model.

Figure 10 comes back to the differences in surface air temperature, but the focus is on July–August and August–September. It first indicates that soil moisture remains a major boundary forcing during the whole summer season since the temperature signal remains strong in GC and GG compared to the JJA differences shown in Fig. 8. It also demonstrates that soil moisture initialization is relevant not

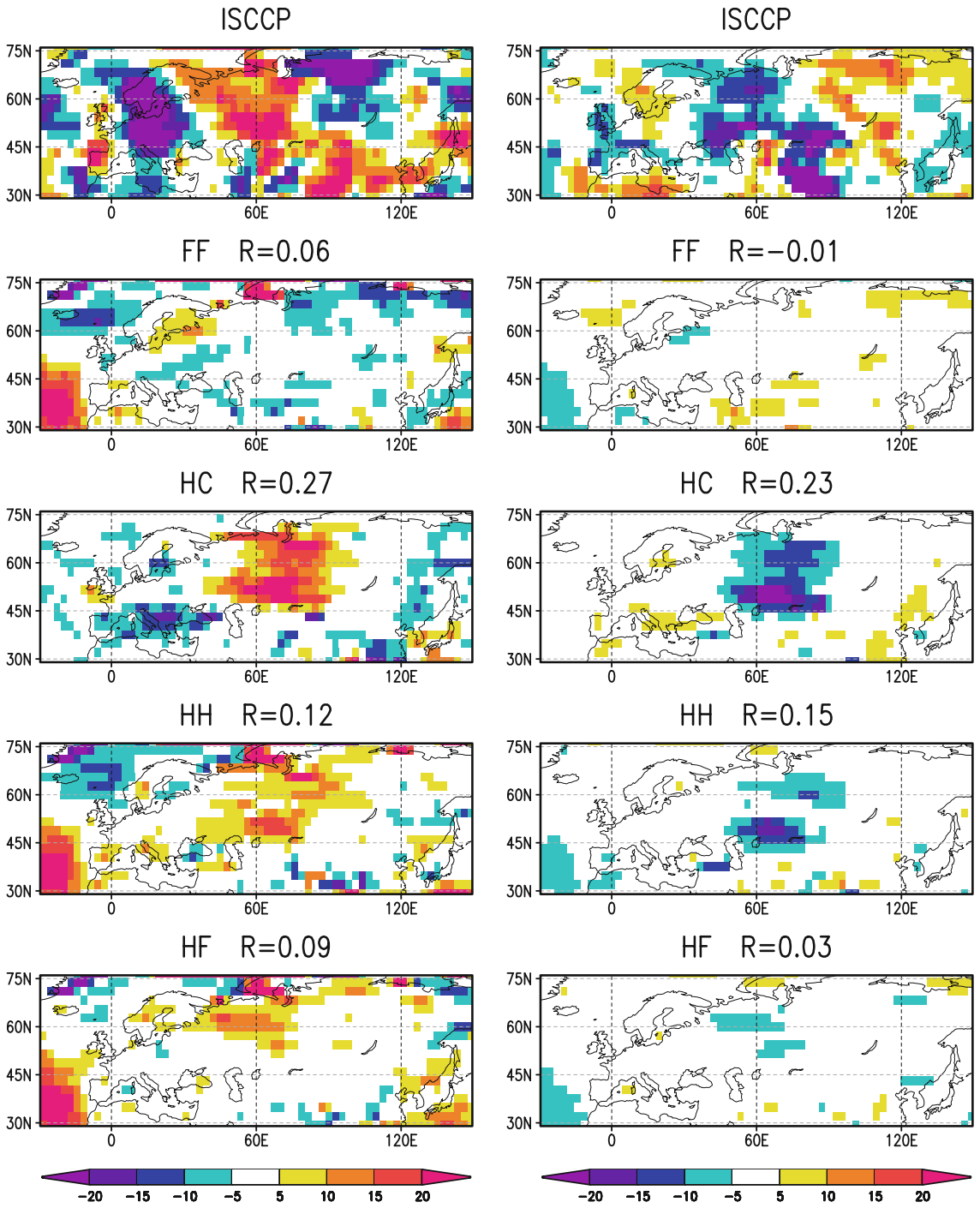

Fig. 12 April to June 1995 minus 1993 differences of surface net shortwave (*left*) and net longwave (*right*) radiation (downward is positive, W/m^2) in FF, HC, HH and HF, respectively. For each experiment, R is the spatial correlation with the upper panel (ISCCP2 climatology)

only at the monthly timescale, but also at months 2–3 or 3–4, since the temperature signal vanishes only at the end of the 4-month hindcast in GF, in line with the predictability of soil moisture shown in Fig. 3.

Finally, it should be noticed that summer 1992 follows the 1991 Pinatubo eruption. While the indirect radiative impact of the eruption (i.e., mainly through the SST boundary conditions) has been considered in our experiments, volcanic aerosols and their direct impacts on radiation and water cycle have been neglected. The model is therefore not supposed to fully capture the 1992 minus 1987 contrast in temperature and precipitation.

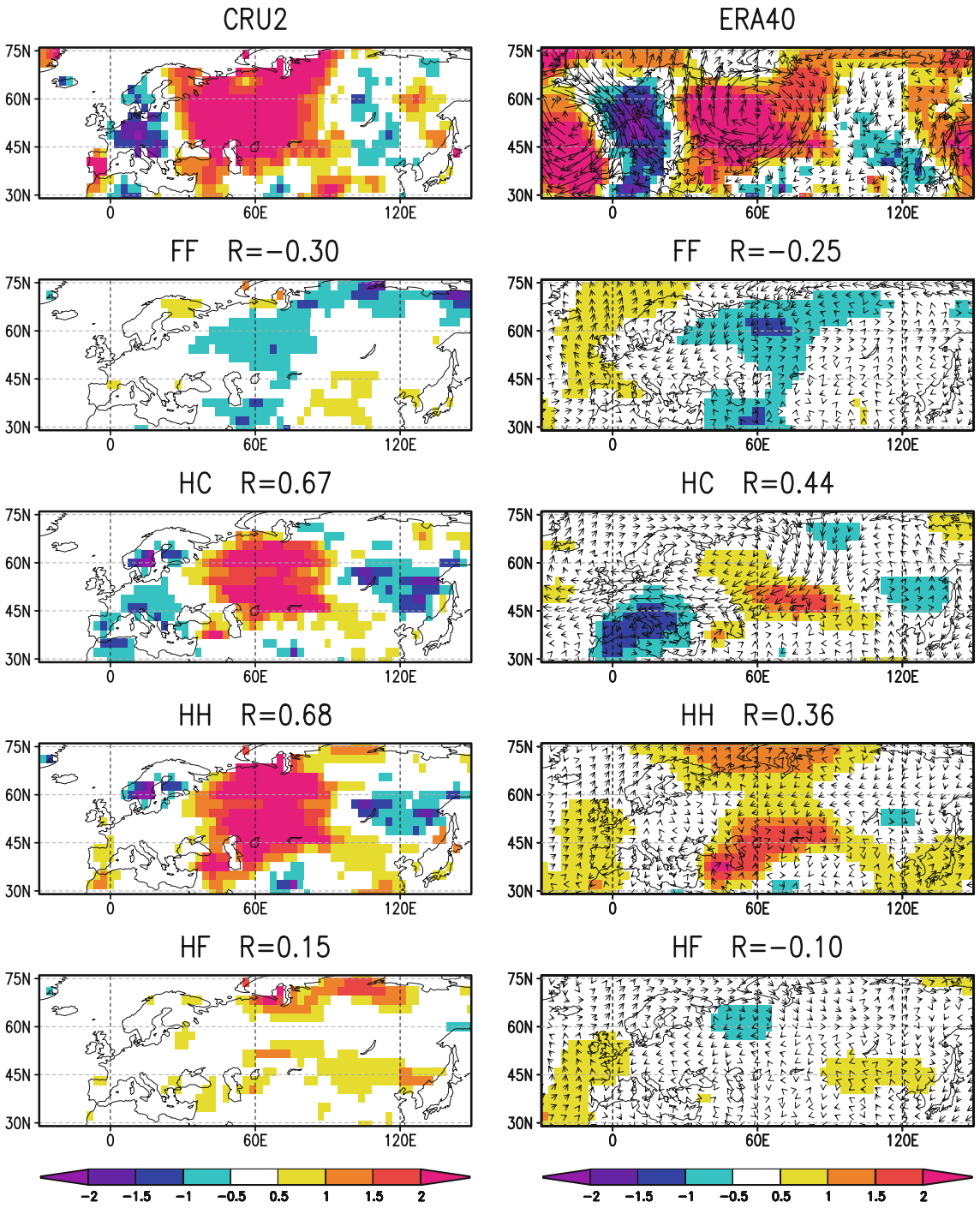

Fig. 13 April to June 1995 minus 1993 differences of temperature (K) at 2 m (*left*) and 850 hPa (*right*) in FF, HC, HH and HF, respectively. For each experiment, R is the spatial correlation with the upper panel (CRU2 climatology or ERA40 reanalysis). *Left panels* horizontal wind vector anomalies at 850 hPa are superimposed on temperature differences

4.3 AMJ 1995 minus AMJ 1993

Moving to the contrasted snow cover observed over central Eurasia between spring 1993 and 1995, Fig. 11 first compares the seasonal mean differences in the latent/sensible heat flux simulated in FF, HC, HH and HF. The GSWP-2 reanalysis shows significant anomalies south of the maximum snow deficit, that is in the transition zone between snow-free and snow-covered areas. In this region, an earlier retreat of the winter snow cover is associated with a

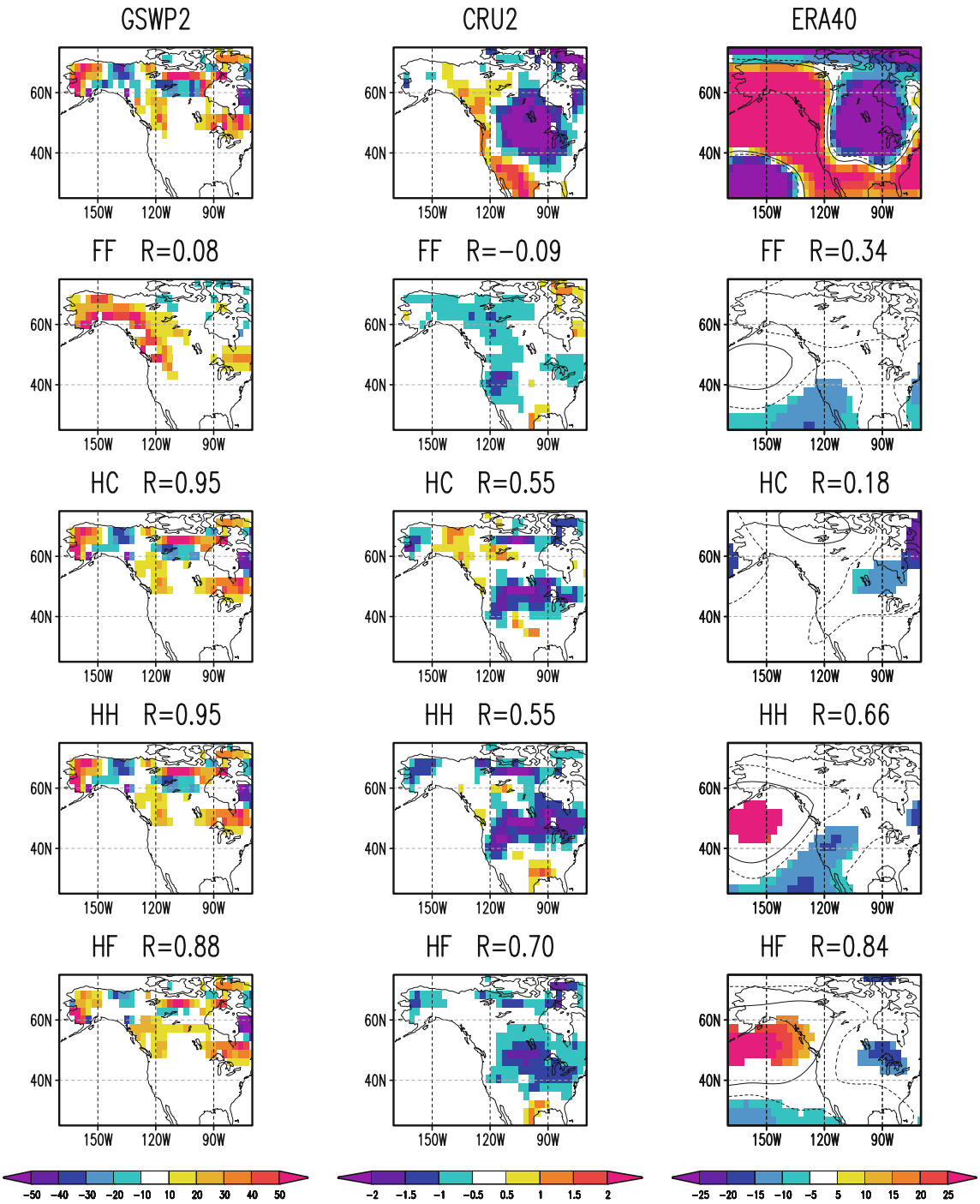

Fig. 14 April to June 1989 minus 1988 differences of snow mass (*left*, kg/m^2) surface air temperature (middle, K) and 500 hPa geopotential height (*right*, m) over North America in FF, HC, HH and HF, respectively. For each experiment, R is the spatial correlation with the upper panel (GSWP2, CRU2, and ERA40, respectively). For geopotential height, *black contours* denote the ±5 m *isolines and shading* show simulated differences that are statistically significant at a 5% level

springtime soil moisture deficit (not shown), which leads to positive (negative) latent (sensible) heat flux anomalies. Such anomalies are captured in the nudged experiments, but not in the seasonal hindcasts. In the northern region, the nudged experiments show an increase in surface evaporation, which is much more pronounced than in the GSWP-2 reanalysis. It compensates for a decrease in snowmelt (not shown) which is strongly overestimated in the nudged experiments because of the artificial imbalance introduced in the snow mass budget.

Moving to surface radiation (Fig. 12), the ISCCP climatology shows increased net solar radiation in the region where the earlier retreat of the snow cover leads to a strong decrease in surface albedo. Such anomalies are well reproduced in the nudged experiments, but much weaker in the seasonal hindcasts. In line with the associated soil moisture deficit (not shown), the simulated increase in net solar radiation is reinforced by a decrease in total cloud cover that is also found in the ISCCP climatology (not shown). The warming at the land surface and the reduced cloudiness induce a radiative cooling that is relatively consistent between ISCCP and the nudged experiments. Again, the signature is much weaker in the seasonal hindcasts, in line with the predicted snow mass deficit that is confined to the northern latitudes (Fig. 5).

Figure 13 compares the simulated and observed differences in temperature both at 2 m and 850 hPa. Consistent with the response of the surface energy budget, the CRU climatology and ERA40 reanalysis show a strong warming over northern and central Eurasia. In contrast with the control experiment, the nudged experiments are able to capture the surface warming, but the signal disappears at 850 hPa in the northern part of the domain where the presence of snow in spring leads to a (too?) strong stratification of the lower troposphere in the model. Moreover, the surface warming vanishes in the seasonal hindcasts (HF) despite the relative persistence of the initial snow mass anomalies north of 60°N (Fig. 5). Finally, the nudged experiments with climatological SST (HC) show a wind response at 850 hPa that is somewhat consistent with the ERA40 reanalysis and suggest that persistent snow anomalies are likely to exert a significant influence on the large-scale dynamics.

In summary, the results show a significant climate influence of snow mass anomalies at the regional scale. The strongest signals are found in the transition zone between snow-free and snow-covered areas and are partly associated with a hydrological snow effect whereby an early snowmelt leads to a soil moisture deficit in spring. A weak dynamical response and a significant cloud feedback are simulated in the nudged experiments that are somewhat consistent with the observations. In contrast with soil moisture anomalies, no impact is noted on precipitation (not shown) and no clear signal is found in the seasonal hindcast experiments.

This rather pessimistic conclusion about the snow contribution to seasonal predictability must be tempered. More encouraging results have been found over North America, for example for the difference between spring 1988 and 1989 (Fig. 14). In this case, the hindcast experiments show surprisingly the best correlations with the observed differences in both surface air temperature and mid-tropospheric geopotential height. This is not only true for the whole AMJ season, but also for each individual month (not shown). Note however, that the predictability found in the 1989 minus 1988 differences mainly originates from the 1989 anomalies (relative to the 1986–1995 climatology), while the snow nudging has a weaker impact in spring 1988 (in line with the weaker snow anomalies). Winter 1988/1989 experienced a large shift in the northern hemisphere extratropical circulation that has been partly attributed to snow cover anomalies observed in early winter over Eurasia (Watanabe and Nitta 1998). Our results (HC and HH vs. FF) are consistent with this study and suggest a strong Eurasian snow forcing of the winter 1988/1989 extratropical circulation (not shown). The atmospheric response found in spring 1989 over North America may therefore be related not only to the regional snow anomalies, but also to a remote influence of the winter Eurasian snow cover. Such teleconnexions induced by snow anomalies have been documented both in winter (i.e., Cohen and Entekhabi 1999) and summer (i.e., Peings and Douville 2008), and several mechanisms have been proposed for the delay between the snow anomalies and their atmospheric impact: a tropospheric-stratospheric pathway involving the excitation of Rossby waves and their interaction with the mean flow from fall to winter, a land hydrology pathway involving soil moisture anomalies and their impact on the land–sea temperature contrast from spring to summer. Such hypotheses are still a matter of debate and are beyond the scope of the present study.

5 Summary and discussion

Seasonal climate predictability and seasonal forecasting rely on the atmospheric sensitivity to its lower (ocean and land) and upper (stratosphere) boundary forcings and on the possible predictability of these boundary forcings. The development of operational DSP systems has been motivated by the increasing ability of coupled ocean-atmosphere GCMs to simulate and predict El Niño Southern Oscillation (ENSO) events in the tropical Pacific and their global teleconnections. Nevertheless, the sporadic nature of the ENSO events and their limited impact on extratropical climate are major obstacles for providing useful seasonal forecasts on a regular and global basis. Moreover, many coupled GCMs still show serious deficiencies in simulating realistic ENSO teleconnections (Joly et al. 2007). Besides improving the coupled ocean–atmosphere models, it is therefore important to look for other potential sources of long-range atmospheric predictability.

Though land surface anomalies are generally less persistent than tropical SST anomalies, they have significant impacts on regional climate that are presumably easier to capture than the remote SST effects. The GLACE

intercomparison project has been a first stage in the evaluation of the land–atmosphere coupling and its potential contribution to climate variability. Nevertheless, the focus was on subseasonal rather than seasonal timescale, mainly on soil moisture and solely on the boreal summer season. There is therefore a need for exploring the land surface contribution to seasonal predictability in a more comprehensive and systematic way.

This is the reason why GLACE will be followed by an ambitious GLACE-2 project (http://glace.gsfc.nasa.gov) that is supported by WCRP (2008). The aim is to analyse the impact of GSWP-2 versus random initial land surface conditions in ensembles of 2-month atmospheric hindcasts over the 1986–1995 summer seasons. The experiment design is therefore close to the one used in the present study. We recognize the need of a multi-model assessment of land surface initialization for improving seasonal forecasting. Nevertheless, it is also important to conduct parallel pilot studies in order to analyse the results of a particular model in more detail.

The present study compares the relative contribution of soil moisture and snow mass to seasonal climate predictability. Though the focus was mainly on the Eurasian continent, similar results were obtained over North America and the main findings can be summarized as follows:

- Soil moisture and snow mass anomalies can be predicted a few months ahead when they show a sufficient magnitude and spatial extent.
- The contribution of soil moisture to boreal summer predictability is not only found over North America, but also over Europe in line with recent observational and numerical studies.
- The contribution of snow cover to boreal spring predictability is also potentially relevant, but is less clear than for soil moisture and deserves further analysis given the possible remote impacts of snow anomalies.
- Both contributions should not be neglected given the weak (though possibly underestimated) SST contribution to extratropical predictability in current atmospheric GCMs.
- Both contributions are not confined to simple changes in surface evaporation (soil moisture) or surface albedo (snow), but involve changes in the various components of the surface energy budget.
- Both contributions could also involve large-scale dynamics and cloud feedbacks that deserve more detailed validation studies.

While such results claim for a better land surface initialization in operational DSP systems, they need to be confirmed by the GLACE-2 project. Moreover, several additional issues have to be explored. First of all, soil moisture and snow depth are not the only land surface variables that represent a potential source of long-range predictability. Recently, subsurface soil temperature was found to increase surface air temperature variability and memory, but with a negligible impact on predictability in many regions of the world, particularly during boreal summer season (Mahanama et al. 2008). Vegetation is also likely to amplify climate variability at least at the multi-decadal timescale, but its role at the seasonal timescale is still uncertain and deserves further statistical (i.e., Liu et al. 2006) and numerical (i.e., Gao et al. 2008) studies. Finally, floodplains or groundwaters also show a significant low-frequency variability that could have regional impacts on interannual climate variability (Bierkens and van den Hurk 2007), but have not yet been included in most LSMs and have to be parametrized in a sufficiently robust way to be coupled with global atmospheric GCMs (i.e., Decharme et al. 2008).

The lack of observational data and the current limitations of land surface data assimilation systems is another important issue (see for instance Houser et al. 2004 for a review about terrestrial data assimilation). For this reason, the forcing of LSMs with meteorological analyses remains an interesting strategy to produce land surface reanalyses. It should be however, emphasized that GSWP-2 represents an upper limit of what can be done routinely given the difficulty to get accurate real-time precipitation analyses in many regions of the world. Current efforts are devoted to assimilate satellite data in LSMs and/or NWP models and should provide improved global high-resolution soil moisture and snow mass datasets in the near future. Nevertheless, it will be necessary to wait still for many years before testing how useful such products are for understanding climate variability and initializing dynamical seasonal forecasts. Meanwhile, land surface reanalyses such as our GSWP dataset could be extended to a longer period (using for example the Princeton atmospheric forcings proposed by Sheffield et al. 2006) to repeat our seasonal hindcast experiments and get a more robust assessment of the impact of land surface initialization on model skill.

Other issues are related to the fact that most sensitivity studies aimed at exploring the land surface influence on climate variability have been based on atmospheric GCMs driven by prescribed SST. On the one hand, such an experiment design assumes that ocean variability is generally considered to be insensitive to land surface variability. This hypothesis is only valid if the land surface contribution to atmospheric variability is a second-order effect or at least confined to the continental areas, which is still a matter of debate (i.e., Hu et al. 2004). On the other hand, the use of prescribed SST can lead to an overestimation of atmospheric sensitivity to land surface

perturbations given the fact that possible negative SST feedbacks are thereby neglected (i.e., Douville 2005). This is the reason why the comparison of coupled ocean-atmosphere hindcasts to atmospheric only hindcasts driven by observed SST would be valuable within the on-going GLACE-2 intercomparison project.

Acknowledgments This work was supported by the ENSEMBLES European project (contract GOCE-CT-2003-505539). Most 2D figures have been prepared using the GrADS software. The author wish to thank the anonymous reviewers for their helpful comments. Thanks are also due to Sophie Tyteca and Sebastien Conil for technical support.

References

Bierkens MFP, van den Hurk BJJ (2007) Groundwater convergence as a possible mechanism for multi-year persistence in rainfall. Geophys Res Lett 34:L02402

Brown RD, Brasnett B, Robinson D (2003) Gridded North American monthly snow depth and snow equivalent for GCM evaluation. Atmos Ocean 41:1–14

Cohen J, Entekhabi D (1999) Eurasian snow cover variability and Northern Hemisphere climate predictability. Geophys Res Lett 26:345–348. doi:10.1029/1998GL900321

Conil S, Douville H, Tyteca S (2007) The relative role of soil moisture and SST in climate variability explored within ensembles of AMIP-type simulations. Clim Dyn 28:125–145. doi:10.1007/s00382-006-0172-2

Conil S, Douville H, Tyteca S (2008) Contribution of realistic soil moisture initial conditions to boreal summer predictability. Clim Dyn. doi:10.1007/s00382-008-0375-9

Decharme B, Douville H (2007) Global validation of the ISBA subgrid hydrology. Clim Dyn 29:21–37. doi:10.1007/s00382-006-0216-7

Decharme B, Douville H, Prigent C, Papa F, Aires F (2008) A new global river flooding scheme: off-line validation over South America. J Geophys Res 113:D11110. doi:10.1029/2007JD009376

Delworth T, Manabe S (1989) The influence of soil wetness on near-surface atmospheric variability. J Clim 2:1447–1462

Dirmeyer P (2000) Using a global soil wetness dataset to improve seasonal climate simulation. J Clim 13:2900–2922. doi:10.1175/1520-0442(2000)013<2900:UAGSWD>2.0.CO;2

Dirmeyer P (2005) The land surface contribution to the potential predictability of boreal summer season climate. J Hydrometeorol 6:618–632. doi:10.1175/JHM444.1

Dirmeyer PA, Gao X, Zhao M, Guo Z, Oki T, Hanasaki N (2006) GSWP-2: multi-model analysis and implications for our perception of the land surface. Bull Am Metab Soc 87:1381–1397. doi:10.1175/BAMS-87-10-1381

Doblas-Reyes FJ, Hagedorn R, Palmer TN (2005) The rationale behind the succes of multi-model ensembles in seasonal forecasting. Part II: Calibration and combination. Tellus 57A:234–252

Douville H (1998) Validation and sensitivity of the global hydrologic budget in stand-alone simulations with the ISBA land surface scheme. Clim Dyn 14:151–171. doi:10.1007/s003820050215

Douville H (2002) Influence of soil moisture on the Asian and African monsoons. Part II: interannual variability. J Clim 15:701–720

Douville H (2003) Assessing the influence of soil moisture on seasonal climate variability with AGCMs. J Hydrometeorol 4:1044–1066. doi:10.1175/1525-7541(2003)004<1044:ATIOSM>2.0.CO;2

Douville H (2004) Relevance of soil moisture for seasonal atmospheric predictions: is it an initial value problem. Clim Dyn 22:429–446. doi:10.1007/s00382-003-0386-5

Douville H (2005) Limitations of time-slice experiments for predicting regional climate change over South Asia. Clim Dyn 24:373–391. doi:10.1007/s00382-004-0509-7

Douville H, Chauvin F (2000) Relevance of soil moisture for seasonal climate predictions: a preliminary study. Clim Dyn 16:719–736. doi:10.1007/s003820000080

Douville H, Royer J-F, Mahfouf J-F (1995) A new snow parameterization for the Météo-France climate model. Part-I: Validation in stand-alone experiments. Clim Dyn 12:21–35. doi:10.1007/BF00208760

Douville H, Chauvin F, Broqua H (2001) Influence of soil moisture on the Asian and African monsoons. Part I: Mean monsoon and daily precipitation. J Clim 14:2381–2403

Douville H, Conil S, Tyteca S, Voldoire A (2007) Soil moisture memory and West African monsoon predictability: artefact or reality? Clim Dyn 28:723–742. doi:10.1007/s00382-006-0207-8

Ferranti L, Viterbo P (2006) The European summer of 2003: sensitivity to soil water initial conditions. J Clim 19:3659–3680. doi:10.1175/JCLI3810.1

Gao X, Dirmeyer PA, Guo Z, Zhao M (2008) Sensitivity of land surface simulations to the treatment of vegetation properties and the implications for seasonal climate prediction. J Hydromet 9:348–366. doi:10.1175/2007JHM931.1

Houser P, Hutchinson MF, Viterbo P, Douville H, Running SW (2004) Terrestrial data assimilation. Chapter C.4 of the BAHC synthesis book "Vegetation, Water, Humans and the Climate". Springer, Heidelberg, 545p

Hu Z-Z, Schneider EK, Bhatt US, Kirtman BP (2004) Potential mechanism for response of El Niño-Southern Oscillation variability to change in land surface energy budget. J Geophys Res 109:D21113. doi:10.1029/2004JD004771

Joly M, Voldoire A, Douville H, Terray P, Royer J-F (2007) African monsoon teleconnections with tropical SST in a set of IPCC4 coupled models. Clim Dyn 29:1–20. doi:10.1007/s00382-006-0215-8

Koster R, The GLACE team (2004) Regions of strong coupling between soil moisture and precipitation. Science 305:1138–1140. doi:10.1126/science.1100217

Koster R, Suarez M, Heiser M (2000) Variability and predictability of precipitation at seasonal to interannual timescales. J Hydrometeorol 1:26–46. doi:10.1175/1525-7541(2000)001<0026:VAPOPA>2.0.CO;2

Koster R, Suarez M, Liu P, Jambor U, Berg A, Kistler M, Reichle R, Rodell R, Famiglietti J (2004) Realistic initialization of land surface states: impacts on subseasonal forecast skill. J Hydrometeorol 5:1049–1063. doi:10.1175/JHM-387.1

Kumar A, Yang F (2003) Comparative influence of snow and SST variability on extratropical climate in northern winter. J Clim 16:2248–2261. doi:10.1175/2771.1

Liu Z, Notaro M, Kutzbach J (2006) Assessing global vegetation-climate feedbacks from observations. J Clim 19:787–814

Mahanama SPP, Koster RD, Reichle RH, Suarez MJ (2008) Impact of subsurface temperature variability on surface air temperature variability: an AGCM study. J Hydromet 9:804–815. doi:10.1175/2008JHM949.1

Mahfouf J-F, Manzi AO, Noilhan J, Giordani H, Déqué M (1995) The land surface scheme ISBA within the Météo-France climate model ARPEGE. Part I: Implementation and preliminary results. J Clim 8:2039–2057. doi:10.1175/1520-0442(1995)008<2039:TLSSIW>2.0.CO;2

Notaro M (2008) Statistical identification of global hot spots in soil moisture feedbacks among IPCC AR4 models. J Geophys Res 113:D09101. doi:10.1029/2007JD009199

Palmer T (2005) Preface of the special issue of Tellus on the DEMETER European project. Tellus 57A:217–218

Palmer T, Anderson DLT (1994) The prospect for seasonal forecasting—a review paper. Quaterly J R Metab Soc 120:755–793

Peings Y, Douville H (2008) Influence of the Northern Hemisphere snow cover on the Indian summer monsoon variability in observations and CMIP3 simulations. Clim Dyn (submitted)

Sheffield J, Goteti G, Wood E (2006) Development of a 50-year high-resolution global dataset of meteorological forcings for land surface modeling. J Clim 19:3088–3111. doi:10.1175/JCLI3790.1

Uppala SM, Kallberg PW, Simmons AJ, Andrae U, Da Costa Bechtold V, Fiorino M, Gibson JK, Haseler J, Hernandez A, Kelly GA, Li X, Onogi K, Saarinen S, Sokka N, Allan RP, Andersson E, Arpe K, Balmaseda MA, Beljaars ACM, Van De Berg L, Bidlot J, Bormann N, Caires S, Chevallier F, Dethof A, Dragosavac M, Fisher M, Fuentes M, Hagemann S, Hólm E, Hoskins BJ, Isaksen L, Janssen PAEM, Jenne R, McNally AP, Mahfouf J-F, Morcrette J-J, Rayner NA, Saunders RW, Simon P, Sterl A, Trenberth KE, Untch A, Vasiljevic D, Viterbo P, Woollen J (2005) The ERA-40 re-analysis. Q J R Metab Soc 131:2961–3012. doi:10.1256/qj.04.176

Vautard R and co-authors (2007) Summertime European heat and drought waves induced by wintertime Mediterranean rainfall deficit. Geophys Res Lett 34:L07711. doi:10.1029/2006GL028001

Von Storch H, Zwiers F (1999) Statistical analysis in climate research. Cambridge University Press, Cambridge

Watanabe M, Nitta T (1998) Relative impacts of snow and sea surface temperature anomalies on an extreme phase in the winter atmospheric circulation. J Clim 11:2837–2857. doi:10.1175/1520-0442(1998)011<2837:RIOSAS>2.0.CO;2

WCRP (2008) WCRP Position paper on seasonal prediction. Report from the 1st WCRP Seasonal Prediction workshop, Barcelona, Spain, 4–7 June 2007. ICPO Publication, 127, 23p